

Reversal of Klein reflection in bilayer graphene

Neetu Agrawal (Garg)¹, Sameer Grover², Sankalpa Ghosh² and Manish Sharma¹

¹*Centre for Applied Research in Electronics,*

Indian Institute of Technology Delhi, New Delhi-110016, India and

²*Department of Physics, Indian Institute of Technology Delhi, New Delhi-110016, India*

(Dated: January 26, 2013)

Abstract

Whereas massless Dirac fermions in monolayer graphene exhibit Klein tunneling when passing through a potential barrier upon normal incidence, such a barrier totally reflects massive Dirac fermions in bilayer graphene due to difference in chirality. We show that, in the presence of magnetic barriers, such massive Dirac fermions can have transmission through even at normal incidence. The general consequence of this behaviour for multilayer graphene consisting of massless and massive modes are mentioned. We also briefly discuss the effect of a bias voltage on such magnetotransport.

PACS numbers: 73.43.-f, 81.05.Tp, 72.90.+y, 73.23.-b, 73.63.-b, 78.20.Ci, 42.25.Gy

One of the most remarkable features of electron transport in graphene [1] is that charge carriers are chiral in nature [2] and their degree of chirality changes as the number of layers are varied [3–5]. In monolayer graphene, chirality results in Klein tunneling, namely the perfect transmission of a normally incident electron of energy E through a potential barrier of height V when $E < V$. In contrast to this, for bilayer graphene chirality of a different degree leads to total reflection from the same barrier at normal incidence, a phenomenon often called Klein reflection [6, 7]. Thus, chirality strongly influences coherent ballistic transmission through graphene based heterostructures, a phenomenon which is now experimentally accessible [8–11] and potent with possibilities for new device applications.

For monolayer graphene, it has been shown that the combined effect of an inhomogeneous magnetic field, dubbed as a magnetic barrier, and an electrostatic potential significantly alters ballistic transport of charge carriers. It has already been shown that use of such inhomogeneous magnetic barriers can lead to confinement of chiral electrons as opposed to Klein tunneling [12]. This has subsequently led to a large body of work [13].

In this Letter, we consider the effect of such barriers in the case of bilayer graphene. Fabry-Perot like transmission fringes develop due to scattering of chiral charge carriers from inhomogeneous magnetic barriers in the presence of voltage. By analyzing these fringes, we find that, in contrast to the above discussion on monolayer graphene, it is quite the opposite in bilayer graphene. It is seen that it is possible to actually reverse the Klein reflection of normally incident electrons; namely, the barrier can cause transmission and significantly modifies the observed conductance in bilayer graphene. As we show, this also paves the way of a more generalized understanding of the effect of such magnetic barriers on transport of chiral quasiparticles in multilayer graphene which shares many features of monolayer and bilayer graphene.

The generalized chiral operator of degree J that describes chirality of charge carriers in multiple layer graphene with $ABAB \cdots$ type of stacking is $\hat{h}_{\mathbf{p}}^J = \mathbf{n}_J \cdot \boldsymbol{\sigma}$, where $\mathbf{n}_J = \cos(J\phi)\hat{x} + \sin(J\phi)\hat{y}$, $\phi = \tan^{-1} \frac{p_y}{p_x}$ and $\boldsymbol{\sigma}$ is the two-component Pauli matrix. Monolayer and bilayer graphene are just two cases of this description with $J = 1$ and $J = 2$ respectively. The general Hamiltonian for charged quasiparticles of J -th degree chirality is then

$$H_J \propto |\mathbf{p}|^J h_{\mathbf{p}}^J \quad (1)$$

The above Hamiltonian leads to a pseudo Zeeman effect due to a momentum-dependent

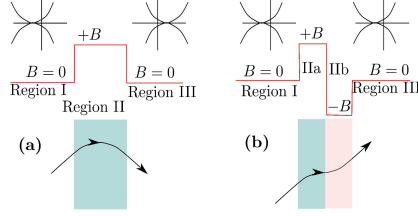


FIG. 1: E - k diagram and electron trajectory in bilayer graphene with (a) magnetic barrier, and (b) barrier + well

pseudo magnetic field $\mathbf{B}_p = |p|^J \mathbf{n}$ [14]. The corresponding eigenstates with definite chirality of degree J are given as

$$|+\rangle = \frac{1}{\sqrt{2}} \begin{bmatrix} e^{-i\frac{J\phi}{2}} \\ e^{i\frac{J\phi}{2}} \end{bmatrix}; \quad |-\rangle = \frac{1}{\sqrt{2}} \begin{bmatrix} e^{-i\frac{J\phi}{2}} \\ -e^{i\frac{J\phi}{2}} \end{bmatrix} \quad (2)$$

These eigenvalues are proportional to $\pm|p|^J$ for the conduction (+) and the valence (-) bands respectively and give both massless and massive Dirac modes for multilayer graphene in general [5]. Eq.(2) also demonstrates how the pseudospin winding number described in Ref.[15] varies with the number of layers.

The upper and lower components of the pseudospinor give the probability amplitude of an electron being in sublattice A and B . A pure scalar potential $V(\mathbf{r})$ cannot flip the pseudospin, namely $\langle \pm | V(\mathbf{r}) | \mp \rangle = 0$, since it couples in the same way with both sublattices. For monolayer graphene with $J = 1$, there is only one massless Dirac mode. Since a scalar potential shifts the Dirac point, to preserve pseudospin, an electron (hole) state outside the potential barrier needs to be matched with a hole(electron) state inside the barrier and that leads to perfect transmission.

The present work discusses bilayer graphene in Bernal stacking, which corresponds to $J = 2$ in Eq.(1) and has one massive Dirac mode. Here also, a scalar potential cannot flip the pseudospin and shifts the Dirac point. However, now the spectrum is parabolic. Hence, a state with \mathbf{p}^2 outside the potential barrier will go to a state with $-\mathbf{p}^2$ inside the barrier to preserve the pseudospin. This requires that a propagating wave outside the barrier should be matched with an evanescent wave inside the barrier leading to total reflection at normal incidence.

Unlike a scalar potential, a vector potential due to a magnetic field $\mathbf{B} = B(x, y)\hat{z}$ couples with the momentum and can flip the pseudospin. In the Landau gauge the vector potential is $\mathbf{A} = A_y(x)\hat{y}$, one can show that when such a magnetic field is present the pseudospin projection angle changes from $J\phi$ to $J\phi'$ where $\phi' = \tan^{-1}(\frac{q_y}{q_x})$, where $q_y = k_y + \frac{eA_y}{\hbar c}$ (cf. Fig.1(a)). Here, we use $\mathbf{k} = \{k_x, k_y\}$ with no magnetic barrier and $\mathbf{q} = \{q_x, q_y\}$ with a magnetic vector potential. The eigenstates are then

$$|+\rangle_B = \frac{1}{\sqrt{2}} \begin{bmatrix} e^{-i\frac{J\phi'}{2}} \\ e^{i\frac{J\phi'}{2}} \end{bmatrix}; \quad |-\rangle_B = \frac{1}{\sqrt{2}} \begin{bmatrix} e^{-i\frac{J\phi'}{2}} \\ -e^{i\frac{J\phi'}{2}} \end{bmatrix}. \quad (3)$$

Scattering between one of the eigenstates in Eq.(2) with $\mathbf{B} = 0$ to one in Eq.(3) for $\mathbf{B} \neq 0$ is now possible as the pseudospin is not necessarily conserved in the presence of a magnetic field. Consequently, perfect Klein reflection upon normal incidence will not take place in bilayer graphene in presence of such a magnetic barrier. We show this by explicitly calculating transmission by a transfer matrix approach [16, 17]. Chiral charge carriers in bilayer graphene obey

$$i\hbar \frac{\partial \Psi(x, y)}{\partial t} = H\Psi, \quad H = \begin{bmatrix} V_1 & \Pi & t & 0 \\ \Pi^+ & V_1 & 0 & 0 \\ t & 0 & V_2 & \Pi^+ \\ 0 & 0 & \Pi & V_2 \end{bmatrix} \quad (4)$$

Here, they are described by a 4-component spinor $\Psi(x, y) = (\Psi_a \ \Psi_b \ \Psi_c \ \Psi_d)^T$ and a 4×4 Hamiltonian in the presence of a magnetic barrier and an electrostatic potential. $\Pi = v_F[p_x + i(p_y + eA/c)]$ with Fermi velocity $v_F = 10^6$ m/s. The magnetic field profile is $\mathbf{B} = B\Theta(x^2 - d^2)\hat{z}$, V_1 and V_2 are the potentials at the two different layers, and t is the tunnel coupling between the two layers. This Hamiltonian reduces to a manifestly chiral symmetric form given in Eq.(1) in the limit $\frac{|E|}{t} \ll 1$, where E is the incident electron energy [4]. $V_1 = (\neq)V_2$ correspond to unbiased (biased) graphene bilayer cases. The stationary solutions $\Psi = \psi(x, y)e^{-\frac{iEt}{\hbar}}$ which obey $H\psi = E\psi$ can be explicitly obtained in the three regions $x < -\frac{d}{2}$ (region I), $-\frac{d}{2} \leq x \leq \frac{d}{2}$ (region II) and $x > \frac{d}{2}$ (region III). In regions I ($j = 1$) and III ($j = 2$) these solutions are propagating as well as evanescent waves. In region II where the magnetic field is finite, stationary solutions are given by parabolic cylindrical functions. We define $\ell_B = \sqrt{\frac{\hbar c}{eB}}$ and $\epsilon_B = \frac{\hbar v_F}{\ell_B}$ as units of length and energy respectively and introduce dimensionless variables $x \rightarrow \frac{x}{\ell_B}$, $v_{1,2} = \frac{V_{1,2}}{\epsilon_B}$ and $\epsilon = \frac{E}{\epsilon_B}$. In regions I and III,

the dispersion relations now become

$$[-q(x)^2 + (\epsilon' + \delta)^2][-q(x)^2 + (\epsilon' - \delta)^2] = (\epsilon'^2 - \delta^2)t'^2$$

Here, $q(x)^2 = q_x^2 + q_y^2$, $q_y(x) = k_y + \text{sgn}(x)\pi\frac{\Phi}{\Phi_0}$, $\epsilon' = \epsilon - v_0$ with $v_0 = (v_1 + v_2)/2 = \frac{V_{\pm}}{\epsilon_B}$ and $\delta = (v_1 - v_2)/2 = \frac{\Delta}{\epsilon_B}$. Also, $\frac{\Phi}{\Phi_0}$ is the total magnetic flux through an area $d\ell_B$ in units of the flux quantum $\Phi_0 = \frac{hc}{e}$, and $\ell_B = \frac{hc}{eB}$ is the magnetic length. For an evanescent wave, $q_x^2 = -\kappa_x^2 < 0$.

We now begin with the case of an unbiased graphene bilayer where $\delta = 0$ and $v_1 = v_2 = v_0$. In regions I and III we set $v_{1,2} = v_0 = 0$. The transmission through such a combination of magnetic barrier and electrostatic barrier can be written using transfer matrices $\mathcal{M}_0(x)$ and $\mathcal{M}_B(x)$, where the subscript 0 (B) defines the region with magnetic field 0 (B). These matrices are given below explicitly.

$$\mathcal{M}_B(x) = \begin{bmatrix} D_{p^+}(z) & D_{p^-}(z) & D_{p^+}(-z) & D_{p^-}(-z) \\ \varepsilon_1^* p^+ D_{p^+-1}(z) & \varepsilon_1^* p^- D_{p^--1}(z) & \varepsilon_1 p^+ D_{p^+-1}(-z) & \varepsilon_1 p^- D_{p^--1}(-z) \\ \varepsilon_2^+ D_{p^+}(z) & \varepsilon_2^- D_{p^-}(z) & \varepsilon_2^+ D_{p^+}(-z) & \varepsilon_2^- D_{p^-}(-z) \\ \varepsilon_1 \varepsilon_2^+ D_{p^++1}(z) & \varepsilon_1 \varepsilon_2^- D_{p^--1}(z) & \varepsilon_1^* \varepsilon_2^+ D_{p^++1}(-z) & \varepsilon_1^* \varepsilon_2^- D_{p^--1}(-z) \end{bmatrix}$$

$$\mathcal{M}_0(x) = \frac{1}{\epsilon'} \begin{bmatrix} \epsilon' e^{iq_x x} & \epsilon' e^{-iq_x x} & \epsilon' e^{-\kappa_x x} & \epsilon' e^{\kappa_x x} \\ [q_x - iq_y(x)]e^{iq_x x} & -[q_x + iq_y(x)]e^{-iq_x x} & i[\kappa_x - q_y(x)]e^{-\kappa_x x} & -i[\kappa_x + q_y(x)]e^{\kappa_x x} \\ -\epsilon' e^{iq_x x} & -\epsilon' e^{-iq_x x} & \epsilon' e^{-\kappa_x x} & \epsilon' e^{\kappa_x x} \\ -[q_x + iq_y(x)]e^{iq_x x} & [q_x - iq_y(x)]e^{-iq_x x} & i[\kappa_x + q_y(x)]e^{-\kappa_x x} & -i[\kappa_x - q_y(x)]e^{\kappa_x x} \end{bmatrix} \quad (5)$$

Here, $z = \sqrt{2}(x + k_y)$, $p^{\pm} = (\gamma_{\pm} - 1)/2$, $\varepsilon_1 = \frac{i\sqrt{2}}{\epsilon}$ and $\varepsilon_2^{\pm} = \frac{\epsilon'}{t'} - \frac{2p^{\pm}}{t'\epsilon}$, and $\gamma_{\pm} = \epsilon'^2 \pm \sqrt{1 + \epsilon'^2 t'^2}$.

The current density expression is obtained as $j_x = v_F \psi^+ \begin{pmatrix} \sigma_x & 0 \\ 0 & \sigma_x \end{pmatrix} \psi$. The transfer matrix through any combination of a scalar and vector potential can now be written in terms of transfer matrices given in Eq.(5) for regions with finite and zero magnetic field. This can then be used to find the transmission. The ratio of current density in region III and the incident current density in region I gives the transmission probability as a function of the angle of incidence $\phi = \tan^{-1} \frac{k_y}{k_x}$.

In Fig.2, the plots in the left column show transmission through a magnetic barrier with increasing strength as a function of the incidence angle and the applied voltage in the barrier

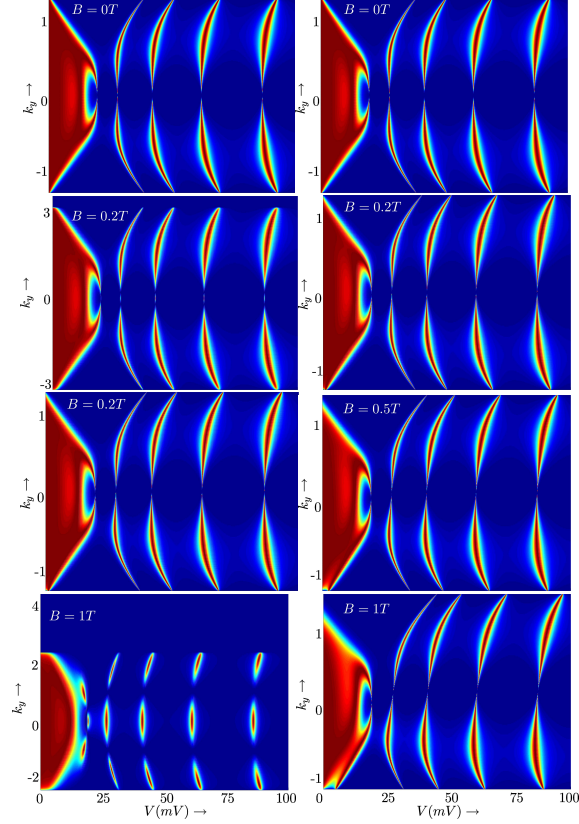


FIG. 2: Transmission T as a function of incidence angle for different fields. (left) Barrier, (right) Barrier+well.

regime. The uppermost figure shows the transmission for $B = 0$, which clearly shows the region of perfect reflection at and around the normal incidence symmetrically placed between two wings of resonant Fabry-Perot fringes. This is a generic feature of transmission through such barriers [8]. As the strength of the barrier increases, a transmission region develops between these two wings due to the effect of magnetic barrier and the resulting transmission also becomes asymmetric. Clearly seen is the disappearance of perfect Klein reflection at normal incidence. The total angular range of transmission however shrinks in the presence of the magnetic barrier since, beyond a certain incident angle, all electron waves suffer total internal reflection. This is an important result of our paper since it shows the exact reason why an inhomogeneous barrier causes Klein reflection to be reversed to transmission for bilayer graphene.

In the right column in Fig.2 is plotted similar transmission through a setup consisting

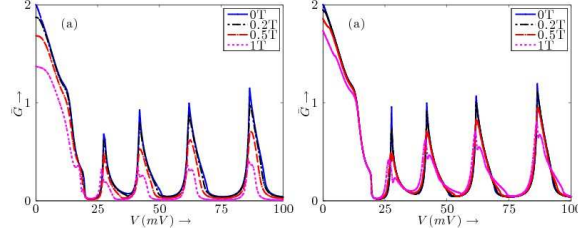


FIG. 3: \bar{G} for different magnetic barrier strengths. (a) Barrier, (b) Barrier+well. $\Delta = 0$, $E = 17meV$ kept constant.

of two magnetic barriers, equal in magnitude and opposite in direction such that the total flux through the region vanishes, as shown in Fig.1. Now, the incident and the transmitted wave vectors are parallel to each other. As a result, the net rotation of the pseudospinor due to the inhomogenous field vanishes and Klein reflection at normal incidence is restored. The bending of the Fabry-Perot fringes can be attributed to the asymmetry in the angular transmission at a given voltage in presence of magnetic barrier + well combination.

We now study the effect of the above transmission on conductance at very low temperatures and for energies close to the Fermi energy in the linear transport regime. To a good approximation, the dimensionless conductance \bar{G} can be written as [13]

$$\bar{G} = \int_{-\frac{\pi}{2}}^{\frac{\pi}{2}} d\phi T(E, \phi) \cos \phi \quad (6)$$

A comparison between the conductance with and without a magnetic barrier in Fig.3 shows that the gaps between the conductance maxima and minima get reduced in the presence of a magnetic barrier. The barrier reflects electrons incident upon it beyond a critical angle and the angular range of transmission shrinks with increasing barrier strength. As a result, the absolute value of conductance maxima comes down. For the barrier+well case, the conductance is slightly higher. This detailed characterization of ballistic transport through magnetic barriers dictated by pseudospin chirality is one of the main results of this work.

The preceding discussion shows how the effect of localized magnetic field on transport of massive Dirac modes encountered in bilayer graphene is very different as compared to that of massless Dirac modes in monolayer graphene. Another important observation can be made by looking at magnetotransport through magnetic barriers for monolayer graphene [12] and the present analysis for bilayer graphene. The same barrier which is reflective for

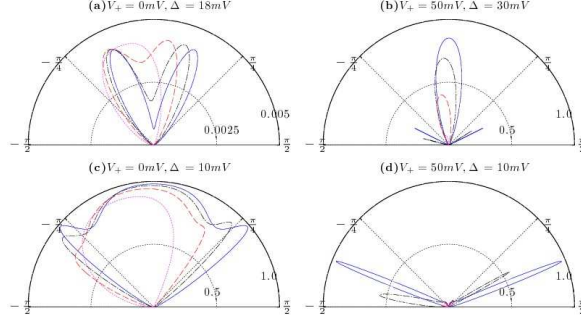


FIG. 4: *Biased bilayer transmission for various V_+ , Δ and magnetic field strengths (colours and lines same as in Fig.3).*

the massless mode is transmissive for the massive mode. The general theory of N -layer graphene predicts the existence of 1 massless and $N - 1$ massive modes for N odd and only massive modes for N even [5]. The magnetic barrier thus can be used to at least partially filter out or to selectively allow a mode.

Finally, we briefly discuss the influence of magnetic barriers on transport through a biased bilayer; i.e., when $V_1 \neq V_2$ in Eq.(4). The effective 2×2 Hamiltonian is

$$\begin{aligned} H_b &= \begin{bmatrix} V_1 & -\frac{v_F^2}{t}(\Pi^\dagger)^2 \\ -\frac{v_F^2}{t}(\Pi)^2 & V_2 \end{bmatrix} \\ &= H_{ub} + \Delta\sigma_z + V_+\mathbf{1} \end{aligned} \quad (7)$$

H_{ub} is the Hamiltonian for the unbiased bilayer given in Eq.(1) for $J = 2$. Thus, bias introduces an additional z component of the pseudo magnetic field. This will try to rotate the pseudospin out of the $x - y$ plane. If Δ is large and the incident energy lies in this gap, the pseudo Zeeman gap will suppress transmission. This is because pseudospin-flipping is energetically costly, a phenomenon that has been experimentally observed [18–21]. The third term in Eq.(7) does not flip the pseudospin. Combining the first two terms, the Hamiltonian can be rewritten as

$$H_b = (\mathbf{n} \cdot \boldsymbol{\sigma}) \sqrt{\Delta^2 + \left(\frac{\hbar^2 q^2 v_F^2}{t} \right)^2}$$

Here, $\boldsymbol{\sigma}$ are three-component Pauli matrices and $\mathbf{n} = (\sin \theta \cos 2\phi', \sin \theta \sin 2\phi', \cos \theta)$ with $\tan \theta = \frac{\hbar^2 q^2 v_F^2}{t\Delta}$. The corresponding pseudospinors $|+\rangle = (\cos \frac{\theta}{2} e^{-i\phi'}, \sin \frac{\theta}{2} e^{i\phi'})^T$ and $|-\rangle =$

$(\sin \frac{\theta}{2} e^{-i\phi'}, -\cos \frac{\theta}{2} e^{i\phi'})^T$ are again eigenstates with definite chirality. Comparing these states with the ones given in Eq.(2), we find that the magnetic barrier gives an in-plane rotation while the bias voltage gives an out-of-plane rotation to the pseudospinor. The two orthogonal rotations can also be given in different spatial regions and have been recently discussed using a Berry phase argument [22] for a pure bias. In this paper, we have considered the case where Δ and \mathbf{B} are non-zero in the same region. If the gap is large and the incident energy lies inside the gap (Fig.4(a)), the transmission as expected is highly suppressed and there is no visible effect of the magnetic barrier. Also, we find that, as long as the incident energy does not lie in the gap (Fig.4(b), (d)) or the gap is too small (Fig.4(c)), the effect of the barrier on the biased and the unbiased bilayers is similar.

This work is supported by grant SR/S2/CMP-0024/2009 of DST, Govt. of India. One of the authors (NA) acknowledges support from CSIR, Govt. of India.

-
- [1] A.H. Castro Neto *et al*, Rev. Mod. Phys. **81**, 109 (2009).
 - [2] M.I. Katsnelson and K.S. Novoselov, Sol. St. Comm. **143**, 3 (2007).
 - [3] K. S. Novoselov *et al.*, Nat. Phys. **2**, 177 (2006);
 - [4] E. McCann and V.I. Fal'ko, Phys. Rev. Lett. **96**, 086805 (2006).
 - [5] H. Min and A.H. MacDonald, Phys. Rev. B **77**, 155416 (2008); H. Min and A.H. MacDonald, Prog. Theor. Phys. Suppl. **176**, 227 (2008).
 - [6] K.S. Novoselov *et al.*, Nat. Phys. **2**, 620 (2006).
 - [7] S. Park and H.-S. Sim, Phys. Rev. Lett. **103**, 196802 (2009).
 - [8] A.V. Shytov, M.S. Rudner, L.S. Levitov, Phys. Rev. Lett. **101**, 156804 (2008); M. Ramezani Masir, P. Vasilopoulos and F.M. Peeters, Phys. Rev. B **82**, 115417 (2010).
 - [9] A.F. Young and P. Kim, Nat. Phys. **5**, 222, (2009).
 - [10] N. Stander, B. Huard, and D. Goldhaber-Gordon, Phys. Rev. Lett. **102**, 026807 (2009).
 - [11] A.F. Young and P. Kim, Ann. Rev. Cond. Matt. Phys. **2** 1-20 (2010).
 - [12] A. De Martino, L. Dell'Anna, R. Egger, Phys. Rev. Lett. **98**, 066802 (2007).
 - [13] M. Ramezani Masir, P. Vasilopoulos, A. Matulis and F.M. Peeters, Phys. Rev. B **77**, 235443 (2008). S. Ghosh and M. Sharma, J. Phys. Cond. Matt. **21**, 292204 (2009); M. Sharma and S. Ghosh, J. Phys. Cond. Matt. **23**, 055501 (2011); L. Dell'Anna and A. De Martino, Phys. Rev.

- B **80**, 155416 (2009); L Dell’Anna and A. De Martino, Phys. Rev. B **79**, 045420 (2009) ; Y.P. Bliokh, V. Freilikher and F. Nori, Phys. Rev B **81**, 075410 (2010)
- [14] A.K. Geim and A.H. MacDonald, Phys. Today **60**, 35 (2007)
- [15] C.-H. Park and N. Marzari, arXiv:cond-mat/1105.1159 (2011).
- [16] M. Ramezani Masir, P. Vasilopoulos and F.M. Peeters, Phys. Rev. B **79**, 035409 (2009) ; M. Ramezani Masir et al., App. Phys. Lett. **93**, 242103 (2008).
- [17] J. Nilsson, A.H. Castro Neto, F. Guinea and N.M.R. Peres, Phys. Rev. B **76**, 165416 (2007) ; M. Barbier, P. Vasilopoulos, F.M. Peeters and J.M. Pereira, Phys. Rev. B **79**, 155402 (2009).
- [18] T. Ohta *et al.*, Science **313**, 951 (2006)
- [19] E. V. Castro *et al.*, Phys. Rev. Lett. **99**, 216802 (2007).
- [20] J. B. Oostinga *et al.*, Nat. Mater. **7**, 151 (2008).
- [21] Y. Zhang *et al.*, Nature **459**, 820 (2009).
- [22] S. Park and H.-S. Sim, arXiv:cond-mat/1103.3331 (2011).

$B = 0.5T$

$k_y \rightarrow$

2

0

-2

